INSTITUTE OF PHYSICS PUBLISHING NETWORK: COMPUTATION IN NEURAL SYSTEMS

Network: Comput. Neural Syst. **13** (2002) 487–501 PII: S0954-898X(02)53151-1

Recovery of hidden information through synaptic dynamics

Misha I Rabinovich[1], R D Pinto[1], Henry D I Abarbanel[2,5], Evren Tumer[3], Gregg Stiesberg[3], R Huerta[1,4] and Allen I Selverston[1]

[1] Institute for Nonlinear Science, University of California, San Diego La Jolla, CA 92093-0402, USA
[2] Department of Physics, Marine Physical Laboratory (Scripps Institution of Oceanography), and Graduate Program in Neuroscience, University of California, San Diego La Jolla, CA 92093-0402, USA
[3] Department of Physics and Institute for Nonlinear Science, University of California, San Diego La Jolla, CA 92093-0402, USA
[4] GNB. ETS Ingeniería Informática, Universidad Autónoma de Madrid, Spain

E-mail: hdia@jacobi.ucsd.edu

Received 5 March 2001, in final form 3 May 2002
Published 20 September 2002
Online at stacks.iop.org/Network/13/487

Abstract

The role of synaptic dynamics in processing neural information is investigated in a neural information channel with realistic model neurons having chaotic intrinsic dynamics. Our neuron models are realized in simple analogue circuits, and our synaptic connections are realized both in analogue circuits and through a dynamic clamp program. The information which is input to the first chaotic neuron in the channel emerges partially absent and partially 'hidden'. Part is absent because of the dynamical effects of the chaotic oscillation that effectively acts as a noisy channel. The 'hidden' part is recoverable. We show that synaptic parameters, most significantly receptor binding time constants, can be tuned to enhance the information transmission by the combination of a neuron plus a synapse. We discuss how the dynamics of the synapse can be used to recover 'hidden' information using average mutual information as a measure of the quality of information transport.

1. Introduction

The last decade has produced a wealth of experimental findings and modelling studies enhancing our understanding of the role of synapses in the processing and transmission of information. Synaptic transmission is an important element in information processing, learning and memory in the central nervous systems of animals [1–7]. The dynamics of synaptic action is tuned,

[5] Author to whom any correspondence should be addressed.

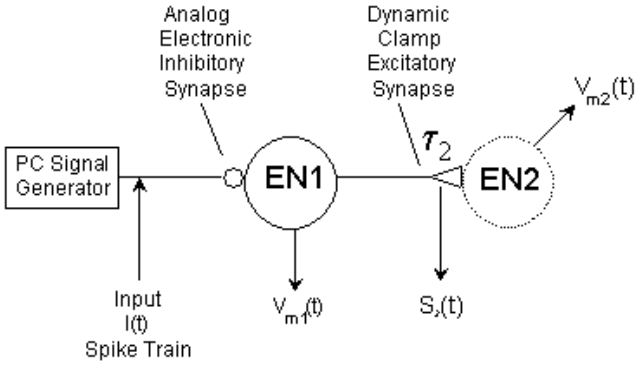

Figure 1. Experimental layout. The input signal consists of unimodal or bimodal Gaussian distributions of ISIs. The input spike sequence $I(t)$ is generated using a digital to analogue converter controlled by a computer (PC). The input signal $I(t)$ inhibits neuron EN1 through an analogue electronic model chemical synapse. EN1 is the presynaptic cell to an excitatory synapse realized through the dynamic clamp protocol. The time series of the excitatory synaptic activation $S_2(t)$, a dimensionless and rescaled $0 \leqslant S_2(t) \leqslant 1$ representation of neurotransmitter binding, is used for the results described in the text. EN2 is just a reader or decoder of the information coming through the synapse. Each experiment consisted of choosing an ISI distribution for the input spike train signal, setting the value of the characteristic time constant of the dynamic clamp synapse, and acquiring a long time series of the input signal $I(t)$, the membrane potential of EN1, $V_{m1}(t)$, and the synaptic activation $S_2(t)$. Signals were digitized at 500 Hz and stored for subsequent analysis.

among other factors, by receptor binding time constants and by thresholds in synaptic processes. In this paper we investigate features of synaptic dynamics operating as a component of a neural information transport 'channel'. The channel we investigate here is shown in figure 1.

Our model information channel, depicted in figure 1, consists of an input current composed of a spike train $I(t)$ with spikes identical in amplitude and with interspike intervals (ISIs) prescribed by the distributions given in what follows. These spikes inhibit a neuron called EN1 through a simple inhibitory synapse whose characteristics are fixed throughout our experiments. This inhibitory synapse is realized in analogue circuitry. From the analogue circuit neuron EN1, the signal goes to an excitatory synapse realized in software using our dynamic clamp program [8]. This permits us to change the characteristics of this synapse during our experiments. The receptor binding percentage $S_2(t)$ at the second synapse sets the level of the postsynaptic current entering the second analogue circuit neuron EN2 after being acted on by the dynamic clamp synapse.

Each electronic neuron is realized using a Hindmarsh–Rose (HR) model [9] for bursting neurons. The synaptic dynamics is represented by a first-order kinetic model of the complicated process of neurotransmitter release and binding to postsynaptic receptors. Here we identify a time constant τ associated with the receptor binding process.

Our analogue electronic model neuron (EN) is based on simple models of bursting, chaotic neurons. These model the typical bursting pattern of cortical neurons [10, 11]. We used bursting neurons because it has been suggested that bursts enhance the release of the neurotransmitter [12, 13]. The EN used in our experiments has been shown (1) to have realistic membrane voltage activity, (2) to be able to replace a biological neuron in a damaged biological network and in doing so restore the functional activity of the network [10], and (3) to reproduce, when interacting in pairs, the details of our observations on coupled biological neurons [14, 15]. The realistic neural activity of the EN has, thus, been quite thoroughly tested.

The detailed equations for our neurons and synapses are discussed below. Each neuron is described by an equation for the membrane voltage and three other variables corresponding to

a 'fast' current, a 'slow' current and an even slower variable associated with slow uptake and release of calcium in the cell. The synapses are described by a dimensionless, neurotransmitter induced, receptor binding factor $S(t)$, $0 \leqslant S(t) \leqslant 1$.

We explore this channel by sending a spike train $I(t)$ into the first synapse whose simplified first-order dynamics is described below. The parameters of the analogue inhibitory synapse were set so that every time there was a spike in the input signal $V_{spike}(t)$, itself proportional to $I(t)$, a negative pulse of amplitude 1.5 V was sent to EN1. In the electronic synapse the time constant τ_1 was fixed at 15 ms. The membrane voltage $V_{m1}(t)$ from EN1 comes to the second synapse and via the dynamics of $S_2(t)$ produces the postsynaptic current $g_2 S_2(t)(V_{m2}(t) - V_{rev2})$ entering neuron EN2.

Using the language of information theory [16] we will show that the total amount of information transmitted through the synaptic dynamics is strongly dependent on the time constant for receptor binding. We will argue that the synapse is able to recover information that was hidden during the first stage of transmission because of the complex temporal dynamics of the chaotic bursting model neuron EN1 [17, 18]. We also show that over an interesting range for the time constant τ_2, the average mutual information (AMI) between an input signal and a synaptic output is *larger* than the AMI between the input signal and the membrane voltage output of the presynaptic bursting neuron. This appears to violate the 'data processing inequality' [19], which states that AMI cannot increase along a chain of information processing elements. The key to understanding this apparent contradiction is that nonlinear neurons can dynamically change their coding space in such a way that some information input to a neuron can become 'hidden' in its output. The main objective of this paper is to reveal that dynamical synaptic action can reveal part of the presynaptic information by tuning itself in a biologically plausible fashion.

The transformation of information from a 'hidden coding space' to a 'visible coding space' by the action of a synaptic dynamics depends strongly on the synaptic characteristics. In particular, the receptor binding time constant plays an essential role. Hidden and 'visible' coding spaces are defined and clarifying examples are given in the appendix.

The postsynaptic neuron EN2 plays the role of reading the message passed along at the synapse, and the parameters of the synapse must be tuned to the properties of the dynamics of the postsynaptic neuron so that the information can be read postsynaptically. However, as we will show, the essential features of information recovery are associated primarily with the presynaptic terminal. The maximization of AMI between the input signal $I(t)$ and fraction of bound receptors $S_2(t)$ as a function of the time constant τ_2 leads us to conjecture an interesting dependence of short-term learning on synaptic time constants rather than solely on the strength of the connections among neurons.

In our results in what follows, the information in $S_2(t)$ is 'decoded' using a threshold decision process. If the signal $S_2(t)$ passes through the threshold value S_{thresh} with a negative derivative, it is an 'event' and a '1' is recorded. If not, a '0' is recorded.

The threshold level S_{thresh} is a function of properties of the postsynaptic neuron, as we discuss below, and can be different for different neurons. Indeed, in [20, 21] the authors discuss the heterogeneity of synaptic dynamics in the brain, and our results may suggest a basis for these observations as the amount of information available to the postsynaptic neuron depends on both S_{thresh} and the receptor binding time constant τ_2.

2. Description of the model

We collect here the full set of dynamical equations for the inhibitory synapse through which the input current $I(t)$ drives neuron EN1, and the synapse is driven by the output potential $V_{m1}(t)$ which is presynaptic to the final neuron EN2. This configuration is depicted in figure 1.

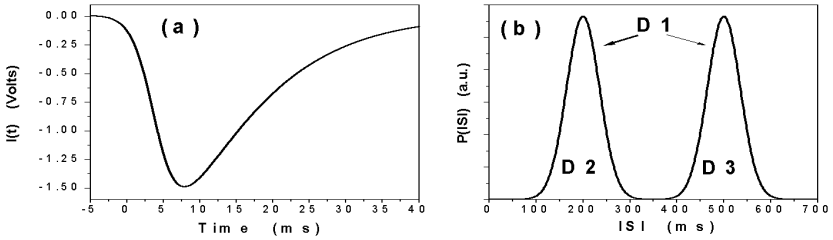

Figure 2. (a) Shape of the signal I_{syn1} that inhibits EN1 when a spike is present in $I(t)$. (b) Distributions of ISIs used to build the input signal. D2 is a unimodal Gaussian distribution with average 200 ms and standard deviation 50 ms, D3 is a unimodal Gaussian distribution with average 500 ms and standard deviation 50 ms, and D1 is a bimodal distribution composed of an equal mixture of D2 and D3.

2.1. Neuron one—realized in analogue circuitry

$$\begin{aligned}\frac{\mathrm{d}V_{m1}(t)}{\mathrm{d}t} &= F(V_{m1}(t), u_{1a}(t)) + I_{DC1} - I_{syn1}(t)\\ \frac{\mathrm{d}u_{1a}(t)}{\mathrm{d}t} &= G_a(V_{m1}(t), u_{1a}(t))\end{aligned} \tag{1}$$

with $a = 1, 2, 3$. $I_{syn1}(t)$ is the synaptic current into neuron one generated by the input spike train with ISIs selected from one of the distributions in figure 2. The equations for the neurons are given below.

2.2. Neuron two—realized in analogue circuitry

$$\begin{aligned}\frac{\mathrm{d}V_{m2}(t)}{\mathrm{d}t} &= F(V_{m2}(t), u_{2a}(t)) + I_{DC2} + g_2 S_2(t)(V_{rev2} - V_{m2}(t))\\ \frac{\mathrm{d}u_{2a}(t)}{\mathrm{d}t} &= G_a(V_{m2}(t), u_{2a}(t))\end{aligned} \tag{2}$$

with $a = 1, 2, 3$. I_{DC} is an injected DC current which sets the environment for the operation of the neuron. $F(V_{m2}(t), u_{2a}(t))$ and $G_a(V_{m2}(t), u_{2a}(t))$ for $a = 1, 2, 3$ govern the dynamics of the variables $(V_{m2}(t), u_{2a}(t))$.

2.3. The Hindmarsh–Rose [14, 21] model neuron

Each of the neurons satisfies the dynamical equations ($j = 1, 2$):

$$\begin{aligned}\frac{\mathrm{d}V_{mj}(t)}{\mathrm{d}t} &= a u_{j1}(t) + b V_{mj}^2(t) - c V_{mj}^3(t) - \mathrm{d}u_{j2}(t) + I_{DCj} - I_{synj}(t)\\ \frac{\mathrm{d}u_{j1}(t)}{\mathrm{d}t} &= e - f V_{mj}^2(t) - u_{j1}(t) - g u_{j3}(t)\\ \frac{\mathrm{d}u_{j2}(t)}{\mathrm{d}t} &= \mu(-u_{j2}(t) + S(V_{mj}(t) + h))\\ \frac{\mathrm{d}u_{j3}(t)}{\mathrm{d}t} &= \nu(-k u_{j3}(t) + r(u_{j1}(t) + l)).\end{aligned} \tag{3}$$

In these equations $a, b, c, d, e, f, g, \mu, S, h, \nu, k, r, e$ and l are constants which embody the underlying current and conductance based dynamics. I_{DCj} and $I_{synj}(t)$ are, respectively, the injected DC current and synaptic input. This HR model captures the observed aspect of neuronal membrane voltage activity while using only four active degrees of freedom [14]. The

detailed relationship between the model parameters and biophysical parameters is still being investigated.

In this polynomial representation of the neural dynamics $V_{mj}(t)$ is the membrane voltage, and $u_{j1}(t)$ represents a 'fast' current. We choose $\mu \ll 1$, so $u_{j2}(t)$ is a 'slow' current. $u_{j3}(t)$ represents an even slower dynamical process ($\nu < \mu \ll 1$) and is included because a slow process, possibly representing the calcium exchange between intracellular stores and the cytoplasm, was found to be required in Hodgkin–Huxley modelling to fully reproduce the observed chaotic oscillations of stomatogastric ganglion neurons [22].

In our analogue circuit realizations of the ENs we used the values $e = 1.0$, $b = 3$, $c = 1$, $d = 0.99$, $e = 1.01$, $f = 5.0128$, $g = 0.0278$, $\mu = 0.002\,15$, $S = 3.966$, $h = 1.605$, $\nu = 0.0009$, $k = 0.9573$, $r = 3$ and $l = 1.619$. These values are estimated from the analogue electronic components, and are known with a 5% tolerance.

EN1 was set to generate tonic spiking behaviour by choosing $I_{DC1} = 7.48$. This is just above the transition to spiking bursting behaviour. EN2 was set into periodic bursting behaviour by setting $I_{DC2} = 2.50$. This is just below the threshold for chaotic bursting. These values were chosen as they emphasize the role synaptic dynamics plays in the information recovery we will demonstrate in what follows.

2.4. Synaptic model

Our model synapse implements the dynamics of chemical synapses using a first-order kinetic model of neurotransmitter release [23, 24]. The current $I_{syn1}(t)$ injected in a postsynaptic cell is determined by the dimensionless, scaled synaptic activation $S_1(t)$; $0 \leqslant S_1(t) \leqslant 1$ via

$$\begin{aligned} I_{syn1}(t) &= g_{syn1} S_1(t)(V_{m1}(t) - V_{rev1}) \\ \tau_1 \frac{\mathrm{d}S_1(t)}{\mathrm{d}t} &= \frac{S_{\infty 1}(V_{in}(t)) - S_1(t)}{S_0 - S_{\infty 1}(V_{in}(t))} \end{aligned} \tag{4}$$

where V_{rev1} is the synaptic reversal potential. $V_{in}(t)$ is the presynaptic voltage which we take proportional to the input current $I(t)$. $V_{m1}(t)$ is the membrane potential of the postsynaptic neuron; here neuron one. τ_1 is the timescale governing receptor binding associated with synapse one. $S_{\infty 1}(V)$ is given by

$$S_{\infty 1}(V) = \begin{cases} \tanh[(V - V_{th1})/V_{slope1}] & \text{if } V > V_{th1} \\ 0 & \text{if } V \leqslant V_{th1} \end{cases} \tag{5}$$

and $S_0 \geqslant 1$.

The dynamics of synapse two, realized in dynamic clamp software, and the synaptic current $I_{syn2}(t)$ entering neuron two are determined by

$$\begin{aligned} I_{syn2}(t) &= g_{syn2} S_2(t)(V_{m2}(t) - V_{rev2}) \\ \tau_2 \frac{\mathrm{d}S_2(t)}{\mathrm{d}t} &= \frac{S_{\infty 2}(V_{m1}(t)) - S_2(t)}{S_0 - S_{\infty 2}(V_{m1}(t))} \end{aligned} \tag{6}$$

where V_{rev2} is the synaptic reversal potential. $V_{m1}(t)$ is the presynaptic voltage from neuron one. $V_{m2}(t)$ is the membrane potential of the postsynaptic neuron; here neuron one. τ_2 is the timescale governing receptor binding associated with synapse one. $S_{\infty 2}(V)$ is given by

$$S_{\infty 2}(V) = \begin{cases} \tanh[(V - V_{th2})/V_{slope2}] & \text{if } V > V_{th2} \\ 0 & \text{if } V \leqslant V_{th2} \end{cases} \tag{7}$$

and $S_0 \geqslant 1$.

In our experiments we implemented the excitatory chemical synapse postsynaptic to EN1 and presynaptic to EN2 using the parameters $g_2 = 350$ nS, $V_{rev2} = -20$ mV, $V_{th2} = -24$ mV and $V_{slope2} = 1$ mV. We varied τ_2 over the range 2 ms $\leqslant \tau_2 \leqslant$ 48 ms in steps of 2 ms. Since we were not interested in changing any parameters of the inhibitory synapse between the input signal generator and EN1, we used an electronic analogue circuit that emulates an inhibitory chemical synapse as described previously. This synapse was simply tuned to provide EN1 hyperpolarizations only for a few incoming spikes.

3. Experiments, information statistics

We built a small, simplified chain of neural processing elements as shown in figure 1. These elements are realized using analogue circuit neural models [14, 18], synaptic models realized by analogue circuits and by our dynamical clamp program [8].

The input signal $I(t)$ is numerically generated and consists of long sequences of spikes with a unimodal or bimodal distribution of ISIs. We used three different ISI distributions (figure 2(b)): D1 consists of a bimodal distribution composed of one 'fast' Gaussian with mean 200 ms and standard deviation 50 ms along with a 'slow' Gaussian centred at 500 ms and also with a standard deviation of 50 ms; D2 consists only of the 'fast' Gaussian; D3, of just the 'slow' Gaussian. The bimodal distribution was inspired in some features of the different spiking/bursting timescales present in real neurons. The shape of each spike is shown in figure 2(a). The program used to generate the input signal first determines the sequence of ISIs according to a chosen distribution and, using a digital to analogue converter, then generates an analogue output voltage corresponding to the model spikes at the times determined by the ISI sequence.

The entropy of a stimulus sequence such as our DK ($K = 1, 2, 3$) tells us how much information, in bits, is brought by that sequence to the receiving neuron. Suppose the sequence is encoded as a set of symbols s_k from a set $S = \{s_1, s_2, \ldots, s_K\}$; this means the waveforms of the stimulus time course $s(t)$ are represented by an alphabet with K elements. (We discuss below the details of our encoding of each of the waveforms $V_{spike}(t)$, $S_1(t)$, $V_{m1}(t)$, $S_2(t)$, and $V_{m2}(t)$.) Words made from this alphabet capture 'events' in the waveform, such as the presence or absence of a spike. If the stimulus symbols have a distribution $P_S(s_k)$, the entropy [16] of this symbol set is given by $H_S = -\sum_{\{s_k\}} P_S(s_k) \log_2[P_S(s_k)]$. We evaluated the entropy H_S(DK) of each of our input or stimulus distributions. It ranges from 7.5 bits for D2 and D3 to about 7 bits for D1. For an isolated Gaussian of standard deviation σ, such as our D2 and D3 distributions, the entropy is

$$H_S \text{ (D2 or D3)} = \tfrac{1}{2}[1 + \log_e(2\pi\sigma^2)], \tag{8}$$

in 'natural' units. For us $\sigma = 50$ ms, so H_S (D2 or D3) is about 7.7 bits. This is the maximum information that could be read at any junction in the subsequent network of neurons and synapses. We show in figure 4 that our neurons and synapses, at best, are able to read about 2.6 bits from this ISI sequence stimulus.

Our 'transmission channel' works reasonably well for the kind of input sequences we choose to transmit; namely, sequences of spikes with various distributions. Would it work better with other sequences? It is quite possible, but the question in neural transmission of information or, equivalently in neural encoding, is how sequences, representative of biologically observed inputs, are treated by the channel. This is quite distinct from the kind of questions a transmission engineer might ask of this channel. For the latter purposes one would seek an encoding of the input information to maximize the information throughput, and success is measured in how close one comes to the entropy of the source. We are given the sequences to transmit, namely representations by spike trains of external stimuli, and need to evaluate how well networks carry

this encoded information. The Gaussian (or bimodal Gaussian) distributions we have chosen represent nearly periodic input with some jitter. Other distributions, in particular Poisson, would be of interest as well.

The conventional framework views a neuron in an information transmission role as a passive element unable to generate its own information. However, real chaotic neurons do generate information. The output from a chaotically oscillating neuron has positive entropy, associated with the instabilities which lead to chaos in the first place [17]. The intrinsic dynamical behaviour of a neuron participating in transferring information depends on the properties of the incoming information signal. For example, a neuron which undergoes subthreshold oscillations may produce action potentials only on receiving an appropriate input.

We analyse information transmission by coding bursts of neural activity, so we have placed EN1 in our experimental set-up close to the threshold of bursting activity. This permits the incoming signal to move the neuron above its bursting threshold, and the outgoing signal from EN1 is quite sensitive to the input. If we were to place EN1, for example, well below threshold, it would be rare for an incoming signal to generate significant output activity. Because EN1 can show chaotic oscillations, its output signal $V_{m1}(t)$ carries information both about the input and the intrinsic dynamics of EN1.

In the scheme of the experiments shown in figure 1 EN2 is exhibited with a dotted curve because all the relevant information processing was contained in the synaptic activation $S_2(t)$. Our earlier paper investigating information transmission [17] noted information recovery using the AMI between the source and the membrane voltage in neuron EN1 AMI(I, V_{m1}) and AMI(I, V_{m2}), the AMI between the source and the membrane potential in EN2. Here we are able to identify the dynamical synapse as the essential element in this process. $V_{m2}(t)$ plays only the role of an 'information reader' which receives the information from the presynaptic neuron. It does not enter our discussion further, though if we wished to know properties of the membrane voltage activity of the postsynaptic neuron, we would have to solve our model equations for $V_{m2}(t)$ and account for its presence in $I_{syn}(t)$. Also the threshold level S_{thresh} used for reading information must be properly tuned to be in accord with properties of the postsynaptic neuron, as we noted earlier.

For each of the three ISI distributions we created 24 data files corresponding to different values of τ_2 in the range 2 ms $\leqslant \tau_2 \leqslant$ 48 ms sampled every 2 ms. Each data series is an hour long, and uses a sampling rate of 500 Hz. We recorded time series for the input signal $I(t)$, for the membrane potential of EN1 $V_{m1}(t)$, for the neurotransmitter release $S_2(t)$, and for the membrane potential of EN2 $V_{m2}(t)$. This sampling rate is too low for studying the detailed shape of spikes but is accurate enough for the detection of spikes, bursts and hyperpolarizations of the ENs.

To characterize the quality of transport of information from a sequence of stimulus symbols $\{s_k\}$ to a location in the network which produces a sequence of response symbols $\{r_l\}$, we use the mutual information between these symbols [16], and then average over this statistic on the symbol sets $\{s_k\}$ and $\{r_l\}$ to determine the AMI.

The mutual information, in bits, between a symbol s_k and a symbol r_l is

$$\log_2\left\{\frac{P_{SR}(s_k, r_l)}{P_S(s_k)P_R(r_l)}\right\}.$$

This answers the question: how much in bits do we learn about a symbol s_k in the stimulus sequence from an observation of a symbol r_l in the response sequence? $P_{SR}(s_k, r_l)$ is the joint distribution of stimulus and response symbols. $P_S(s_k)$ is the distribution of stimulus symbols, and $P_R(r_l)$ is the distribution of response symbols.

The AMI between these two sets of sequences $S = \{s_1, s_2, \ldots, s_K\}$ and $R = \{r_1, r_2, \ldots, r_L\}$ having the joint distribution $P_{SR}(s_k, r_l)$ is

$$\mathrm{AMI}(S, R) = \sum_{\{s_k\},\{r_l\}} P_{SR}(s_k, r_l) \log_2 \left\{ \frac{P_{SR}(s_k, r_l)}{P_S(s_k) P_R(r_l)} \right\}.$$

This answers the question: how much, in bits, do we know about values from the set A from measurements on the set B on the average over all data from each set? $\mathrm{AMI}(S, R) = \mathrm{AMI}(R, S)$. AMI gives us a nonlinear measure of the way in which variations in the output of a neural process are connected with variations in the input.

We calculated the AMI between $I(t)$, and $V_{m1}(t)$, $\mathrm{AMI}(I, V_{m1})$ and the AMI between $I(t)$ and $S_2(t)$, $\mathrm{AMI}(I, S_2)$. If the transmission channel contained only passive elements, then the 'data processing theorem' tells us that $\mathrm{AMI}(I, V_{m1}) \geqslant \mathrm{AMI}(I, S_2)$. Our channel, of course, has dynamical units—the neurons and the synapses—so whether this result holds is a question to be addressed. The failure of this 'theorem' could arise if the dynamics of the channel elements added degrees of freedom not accounted for in the measurements of $V_{m1}(t)$ or $S_2(t)$ alone. That is, we might have to make measurements of other quantities to enlarge the coding space or possibly have to use time delays of these measurements in accord with familiar practice in nonlinear dynamics [25] to achieve the same end.

To implement these calculations we must define a finite coding of the information in each signal. We chose the following: each time series was resampled using time windows of size Δt starting at 2 ms, the minimum size possible as we sampled the data at 500 Hz, then proceeding in steps of 2 ms up to 500 ms. For each Δt we attributed to each window a bit indicating the occurrence, a '1', or the nonoccurrence, a '0', of an event in this window. One 'event' in the stimulus spike train input $I(t)$ is a spike, and, since the input spikes inhibit EN1, we defined one event in V_{m1} as a hyperpolarization of the membrane potential of the neuron. We defined an event in the time course $S_2(t)$ to be a '1' when $S_2(t)$ moves down through S_{thresh}, and a '0' otherwise. So the coding spaces that we consider are 'neuron hyperpolarization' and 'neurotransmitter binding factor moving down through a threshold'.

Both criteria have neurobiological meaning: the first signifies that an initiating spike occurred to start information transmission. As spiking is widely regarded to be the primary means of information transmission, this is critical. The second criterion signifies that the percentage of bound receptors has reached a certain level S_{thresh} above which synaptic current flows to carry neural information forward through the channel. It would have been entirely equivalent to use the rise of $S_2(t)$ through this threshold as an 'event.'

Event detection was carried out by comparing the value of the time series to a selected threshold level: 0.2 V for the spikes in $I(t)$, -42 mV for $V_{m1}(t)$ and different values of S_{thresh} for $S_2(t)$. Starting at the beginning of the strings of resampled and encoded data we built digital words of 8 bits. First we measure bits from the first eight windows of size Δt. Moving one window to the right we built another word of 8 bits, and so on. This word size allows us to deal with the full information content of the input stimuli, D1, D2 and D3, each of which carry about 7.5 bits of information. A word size of eight bits is the minimum we could use to allow the full information in our input spike trains to be represented by any coding scheme. In fact the neural channel we construct passes only about 2.5 bits of the total allowed.

Using the sequence of words from all the signals we calculated the probabilities of finding a specific word in a signal as well as the joint probabilities between each two signals. With these probabilities we used standard procedures [26, 27] to obtain the AMI between I and V_{m1} and between I and S_2. We also calculated the bias corrections [28, 29] for all the information estimations due to limited sampled data. Estimates of AMI and other information theoretic

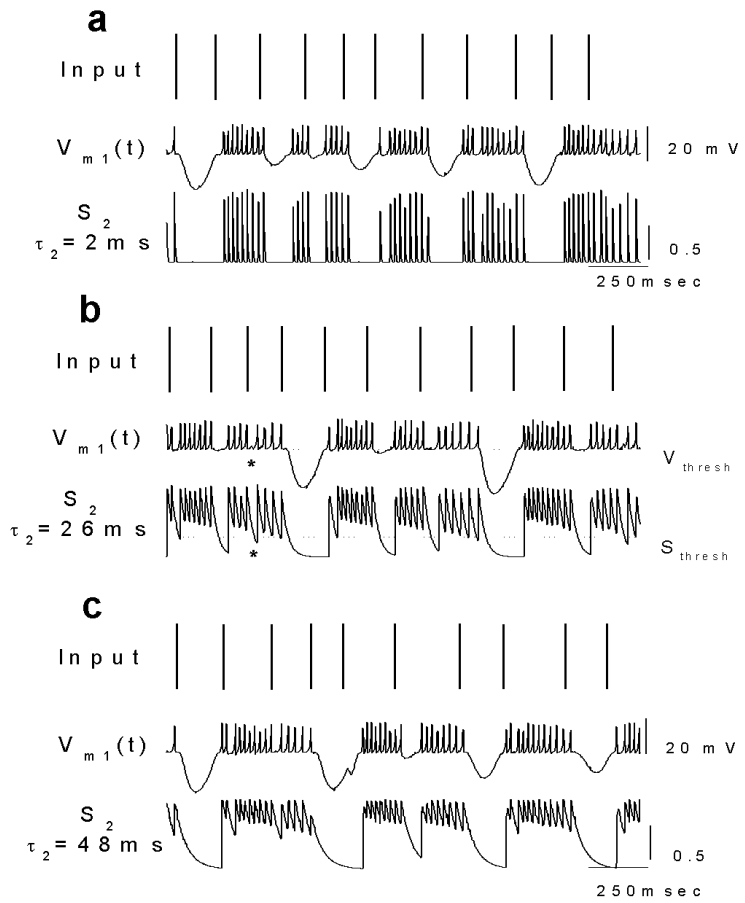

Figure 3. Example time series obtained using D2 as input and various τ_2. (a) $\tau_2 = 2$ ms. (b) $\tau_2 = 26$ ms. (c) $\tau_2 = 48$ ms. In (b) an asterisk marks events that cannot be detected using a threshold level V_{thresh} in $V_{m1}(t)$ but that can be easily detected using a threshold level S_{thresh} for $S_2(t)$. If τ_2 is too small, (a), the information cannot be recovered using threshold levels because the effect of the spikes of the presynaptic cell have large amplitudes in $S_2(t)$, and the current decays so rapidly that it mixes events and the baseline of the spikes at the bottom of the trace; for τ_2 too large, (c), both spikes and events have small amplitudes, and is also more difficult to separate them. This suggests there may be a τ_2 where recovery is maximized.

statistical quantities depend on the number of data. In each calculation we carefully checked that each AMI had become independent of the number of data used in its estimation.

4. Results

Typical experimental time series corresponding to different values for the time constant τ_2 are shown in figure 3. The input distribution for the examples displayed in figure 3 is D2. Looking first at figure 3(a) we see that there is no recovery of the event 'spike in the input' at $\tau_2 = 2$ ms because we are not able to distinguish any specific '$S_2(t)$ event' within the collection of observed spikes. However, the neuron is able to respond to some spikes with a few hyperpolarizations.

When τ_2 is increased to 26 ms, we detect only a few spikes in $V_{m1}(t)$ by seeing a few strong hyperpolarizations, but most of the input spikes are not detected in $V_{m1}(t)$ and thus, they are missing in our coding space; see figure 3(b). On the other hand, the synapse is able to respond to this event by crossing the threshold value most of the time. Therefore, in this example when we record a long time series and calculate AMI(I, V_{m1}) and AMI(I, S_2) we obtain a higher value for the second of these. The '$V_{m1}(t)$ events' are missing because they have been hidden in the nonlinear activity of EN1.

In figure 3(c) we show another case where we have selected $\tau_2 = 48$ ms to qualitatively indicate that the spike detection at the synapse is a little bit worse. This suggests that there may be a τ_2 for which information transmission has a maximum. A qualitatively similar result is found in the study of modelling input signals from spike trains [30].

This example illustrates the basic working mechanisms of our hypothesis that learning and possibly other critical neural processes may be also strongly influenced by receptor binding time constants in synaptic activity rather than only by the maximal conductance values at synapses. To quantitatively establish that the visual impression is correct, we collected large quantities of data and calculated the three AMI values associated with $I(t)$, $V_{m1}(t)$, and $S_2(t)$. In figure 4(a) we present the maximum of AMI(I, S_2) as a function of the synaptic time constant τ_2 and of the coding threshold S_{thresh}. The maximum is taken over the window size Δt used for the encoding and for each distribution it was always found around the same Δt: for the input ISI distribution D1 the maxima were all about $\Delta t = 0.21$ s; for D2, about $\Delta t = 0.14$ s; and for D3, about $\Delta t = 0.4$ s.

Figure 4(b) shows the quantity $\frac{\max\{\text{AMI}(I,S_2)-\text{AMI}(I,V_{m1})\}}{\max\{\text{AMI}\{I,S_2\}\}}$ as a function of the synaptic time constant τ_2 and of the coding threshold S_{thresh}. These calculations were made with the bimodal ISI distribution D1. It is clear that the regions of parameter space (τ_2, S_{thresh}) where the maximum recovery of information occurs roughly coincides with the regions of maximum total information transmitted. For each coding threshold S_{thresh}, the synapse can 'tune' to maximum information recovery by adjusting the time constant τ_2 appropriately. For example, if the threshold S_{thresh} is set at 0.2 a value of $\tau_2 = 15$ ms, will give the maximum information recovery, here about 30% of the total information transmitted. This is a substantial improvement in the ability to transmit information resulting from the action of the dynamical synapse. Quite similar results came from the use of the unimodal distributions D2 and D3.

In figure 5 we present the plots of maximum (over window size Δt) of $\max\{\text{AMI}(I, S_2) - \text{AMI}(I, V_{m1})\}$.

5. Discussion

Using an experimental 'information channel' we have investigated issues associated with how information is transmitted through such a channel when it is composed of dynamically active neurons and synapses. Our channel, shown in figure 1, was constructed from model analogue circuit neurons which have been extensively tested in their membrane voltage activity performance against the similar performance of biological neurons. The synapses entering our network were an inhibitory synapse implemented in an analogue circuit with fixed parameters and an excitatory synapse implemented in software on a PC using our dynamic clamp software [8]. In the latter synapse we were able to vary critical parameters, especially the time constant τ_2.

Our experiments consisted of stimulating the channel through an inhibitory synapse with spike trains of specified ISI distributions, and then recording dynamical variables representing the membrane voltage $V_m(t)$ and the dimensionless, scaled neurotransmitter binding factor $S(t)$ through the rest of the network. Our primary analysis tool was the evaluation of AMI between the input stimulus and the activity at downstream locations in the channel.

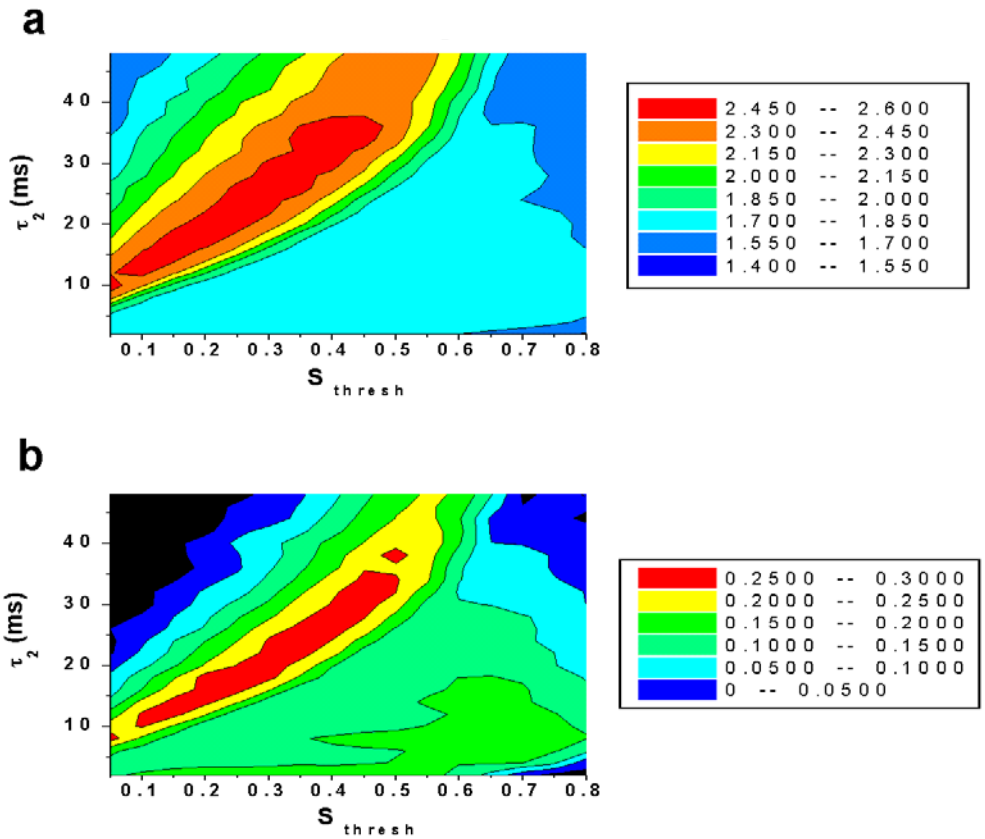

Figure 4. AMI and recovered information. (a) Maximum of AMI(I, S_2) as a function of the synaptic time constant τ_2 and the neurotransmitter threshold S_{thresh}. The maximum is over the window sizes used to encode the data; see the text for details. Outside this region of τ_2 and S_{thresh}, the data processing inequality holds, and no information is 'recovered' by the dynamical synapse. Note that the maximum possible AMI(I, S_2) is the entropy of D1 (about 7.5 bits), so there is some information loss at EN1. (b) $\max\{\text{AMI}(I, S_2) - \text{AMI}(I, V_{m1})\}/\max\{\text{AMI}(I, S_2)\}$ as a function of τ_2 and S_{thresh}. This indicates how much of the total information shown in (a) comes from recovery. The input was D1 for these results.

The essential results of this study are captured in figures 4 and 5 where we show that AMI(I, S_2), the AMI between the spike train stimulus and synaptic output, was larger than AMI(I, V_{m1}), the AMI between the stimulus and membrane voltage presynaptic to the synapse over a large range of time constants τ_2 associated with synaptic properties. This means that the dynamical synapse is able to recover information not readable though observation of its presynaptic membrane voltage.

This result appears to violate the so-called 'data processing theorem' [19], but we have argued that it is a natural consequence of the active dynamics built into the neurons and synapses in our network. It is essential for our results that the dynamical actions of neurons in the network, in particular EN1, can 'hide' information through their chaotic oscillations and that the dynamical actions of synapses in the network can recover this information. The quantitative statement of this is found in figure 5.

Equally important is the fact that figure 5 shows us that this information recovery can be maximized by appropriate choices of synaptic time constants τ_2 properly tuned to the sensitivity

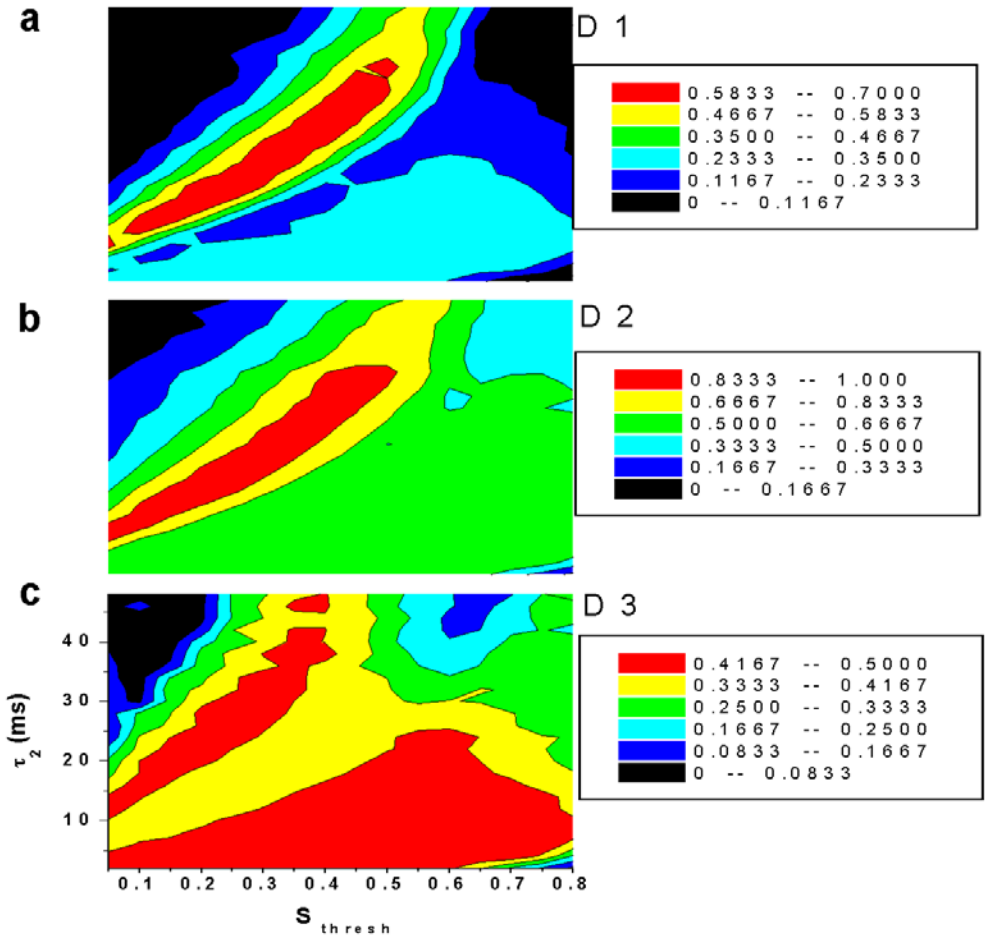

Figure 5. Maximum information recovery $\mathrm{AMI}(I, S_2) - \mathrm{AMI}(I, V_{m1})$ in bits as a function of τ_2 and S_{thresh} for the three ISI distributions used in our experiment. (a) D1, (b) D2, and (c) D3. (a) and (b) have the same scale as (c).

of the postsynaptic cell as represented in the threshold for decisions decoding the information output by the dynamical synapse. Moreover, the values of τ_2 that optimize the information recovery are exactly in the range of the values of neurobiological synaptic time constants.

The latter observation led us to conjecture that observed heterogeneity in neural assemblies [20, 21] may well be expressions of this tuning of various neurons in the networks to achieve maximum information deposition at locations where the information is best used for functional purposes.

From our computations we are led to suggest that a natural 'unit' of information processing in nervous systems is not the component neurons alone, but the well constructed and tuned combination of neurons and their dynamical synapses. Clearly this idea will be clarified by further simulations on networks of increasing complexity and with understandable specific functional goals.

The ability of the dynamical synapse to recover information not readable from $V_{m1}(t)$ hinges on the fact that the stimulus signal and the intrinsic dynamical variation in the neural oscillations are distinct. Thus one is able to separate them dynamically. This feature is used widely in strategies for communication using chaotic waveforms [31].

Finally let us repeat that our calculations have been performed using realistic, well tested, analogue electronic implementations of a reduced model neuron and analogue electronic and computer simulations of the dynamical synapses. These are certainly suggestive of important dynamical processes in nervous systems, but we must proceed to the investigation of the information processes suggested here in hybrid (electronic and biological) networks and, where we are able, in strictly biological networks. This is in progress in our laboratory.

Acknowledgments

R D Pinto was supported by the Brazilian agency Fundação de Amparo à Pesquisa do Estado de São Paulo-FAPESP, under proc. No 98/15124-5. This work was partially supported by the US Department of Energy, Office of Science, through grants No DE-FG03-90ER14138 and No DE-FG03-96ER14592. Partial support was also received through the Office of Naval Research under contracts N0014-00-1-0181 and NN0014-99-1-0647. The National Institute of Health also partially supports this work under grant NS 09322. RH was partially supported by grant MCT BFI2000-0157. HDIA is partially supported by a grant from the National Science Foundation, NSF PHY0097134. We are most appreciative to Attila Szücs and Pablo Varona for numerous discussions regarding this material.

Appendix. Coding space; hidden information

A.1. Coding space

To apply information theory to neural signals we need to define a way to encode the signals found in neural activity. A first step is to define what is an individual 'event'. Usually the definition of an event is related to the kind of observation one is making. Suppose one is applying inhibitory input to a neuron. If the input is able to hyperpolarize the neuron, under certain conditions, an event can be defined as the start of hyperpolarization of the neuron. If the hyperpolarization is sufficient to terminate spontaneous firing or is superimposed upon an already bursting neuron, these events define what we call a bursting code. If one is interested in the role of spikes in neural activity we can establish a spiking code, in which each spike is an event.

An event (hyperpolarization, burst or spike) is detected by comparing the signal with some threshold level and looking for the crossings of the threshold level in a particular direction. We show an example of this coding for the bursting code in figure A.1. We measure a long time series of the membrane potential with total length in time $N\Delta T$. Split the signal into N bins of length ΔT and look in each bin for downward crossings of a threshold V_{thres} by the signal voltage. Every time the signal crosses V_{thres} in the downward direction we attribute a '1' to the bin where the crossing occurred. To the remaining bins, where no downward crossing occurs, we attribute a '0'. In this way a string with N bits is formed.

The next step is to build words of length L bits. Starting from the beginning of the string of N bins, we use L bits to build the first word W_1. Moving ΔT to the right in the string we use the next L bits to create the word W_2. By repeating this process until the full string is used we will form a total of $N - L + 1$ words of L bits each. In this encoding scheme we have an ensemble of $N - L + 1$ items $\{W_1, W_2, \ldots, W_{N-L+1}\}$ each composed of one of 2^L distinct

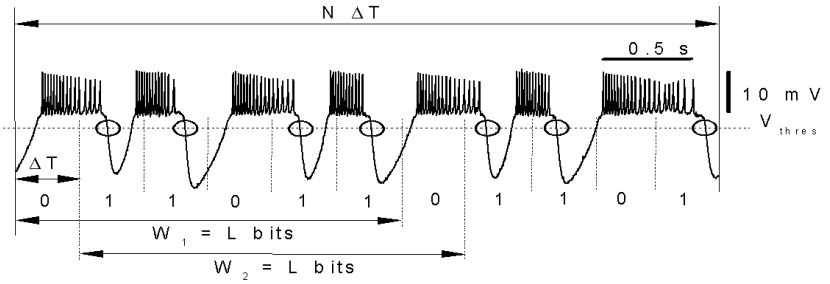

Figure A.1. Encoding a neural signal using a bursting code. A signal of total length $N\Delta T$ is split into N bins of length ΔT. A string of N bits is built by looking in each bin for the occurrence of an event (in this example the crossing of the level V_{thres} by the membrane potential of the neuron during hyperpolarization) these are marked with circles in the figure. If there is an event, we attribute a '1' to the bin, otherwise we attribute a '0' to the bin. Words of length L bits are built starting from the beginning of the string to determine the first word W_1, then moving ΔT to the right to obtain a new word W_2. The process is repeated until $N - L + 1$ words are formed. This gives us an ensemble of $N - L + 1$ words drawn from a selection of 2^L distinct words.

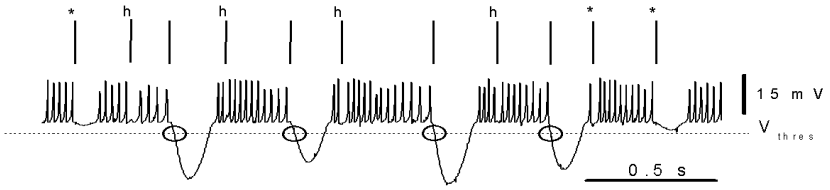

Figure A.2. Information 'hidden' in the neural signal. The upper trace shows a sequence of inhibitory spikes that provide inhibition to a cell whose membrane potential time course is shown in the lower trace. Using a threshold level to detect the events (here, hyperpolarizations of the cell) it is only possible to discriminate some of the information introduced in the cell by the sequence of inhibitory spikes. If we make V_{thres} higher, the effect of the spikes marked with * can be detected, but some of the events (marked with h) are impossible to discriminate using this coding. If one makes V_{thres} high enough to detect all of the incoming spike events, all other spikes in the cell will be misinterpreted as events too. In this case the information about the sequence of inhibitory inputs is not contained in a single code, rather it is stored partly in the bursting code and partly in the spiking code of the cell.

words $\{w_j : w_1, w_2, \ldots, w_{2^L}\}$. Counting the frequency of occurrence of each distinct word w_j we can determine the probability distribution $P_W(w_j)$. If we have two different signals, encoding both signals enables us to calculate the joint probabilities and thus the AMI between the signals.

A.2 'Hidden' information

What happens if the information about some stimulus generates a more complex behaviour in the target cell? For example, suppose a sequence of spikes inhibits a bursting cell. Sometimes the input spike occurs at a moment in which the cell hyperpolarizes, and other times it happens when the neuron is firing and is able only to inhibit the production of a single spike, but no hyperpolarization is observed, as illustrated in figure A.2. If we use the procedure of threshold crossing to detect events, only a small amount of information about the sequence of stimuli can be distinguished in the membrane potential of the cell. If the threshold level is made higher, more events can be detected (these are marked with asterisks), improving the total

input information revealed, but some events (marked with an h) are not detected using the threshold level criteria unless the threshold is put at such a high level that all spike maxima in the target cell will be misinterpreted as events. This is a feature of the method of coarse graining the neural signals.

Now the information contained in the input sequence is still present in the membrane potential of the cell, but it is 'hidden' from the threshold coding method. Part of the information is contained in the hyperpolarizations and part of it is in the spiking behaviour of the cell. The dynamical synapses implemented in this paper are able to recover the information 'hidden' in the spiking of the neuron and to translate it back to a readable threshold coding.

References

[1] Markram H, Gupta A, Uziel A, Wang Y and Tsodyks M 1998 *Neurobiol. Learning Memory* **70** 101–12
[2] Markram H, Tsodyks M, Wang Y and Uziel A 1999 Frequency-dependent synaptic transmission in the neocortex *Advances in Synaptic Plasticity* (Cambridge, MA: MIT Press)
[3] Liaw J S and Berger T W 1996 *Hippocampus* **6** 591–600
[4] Stevens C F and Wang Y 1995 *Neuron* **14** 795–802
[5] Thomson A M 1997 *J. Physiol.* **502** 131–47
[6] Tsodyks M, Pawelzik K and Markram H 1998 *Neural Comput.* **10** 821–35
[7] Destexhe A, Mainen Z F and Sejnowski T J 1994 *J. Comput. Neurosci.* **1** 195–230
[8] Pinto R D, Elson R C, Szucs A, Abarbanel H D I, Rabinovich M I and Selverston A I 2001 *J. Neurosci. Methods* **108** 39–48
The program, source code, user manual and schematics can be downloaded from http://inls.ucsd.edu/∼rpinto
[9] Hindmarsh J L and Rose R M 1984 *Proc. R. Soc.* B **221** 87–102
[10] Mulle C, Madariaga A and Deschênes M 1986 *J. Neurosci.* **6** 2134–45
[11] Johnson S W, Seutin V and North R A 1992 *Science* **58** 665–7
[12] Lisman J E 1997 *T. Neurosci.* **20** 38–43
[13] Prince D 1995 Thirty years among cortical neurons *The Cortical Neurons* ed M J Gutnick and I Mody (Oxford: Oxford University Press)
[14] Pinto R D, Varona P, Volkovskii A R, Szücs A, Abarbanel H D I and Rabinovich M I 2000 *Phys. Rev.* E **62** 2644–56
[15] Elson R, Huerta R, Rulkov N F, Abarbanel H D I and Rabinovich M I 1998 *Phys. Rev. Lett.* **81** 5692–5
[16] Shannon C E and Weaver W 1949 *The Mathematical Theory of Communication* (Urbana: University of Illinois Press)
[17] Eguia M C, Rabinovich M I and Abarbanel H D I 2000 *Phys. Rev.* E **62** 7111–22
[18] Szücs A, Varona P, Volkovskii A R, Abarbanel H D I, Rabinovich M I and Selverston A I 1999 *Neuroreport* **11** 563–9
[19] Borst A and Theunissen F 1999 *Nat. Neurosci.* **2** 947–57
[20] Gupta A, Wang Y and Markram H 2000 *Science* **287** 273–8
[21] Natschlaeger T and Maas W 2001 Finding the key to a synapse *NIPS '2000: Advances in Neural Information Processing Systems 2000* vol 13 (Cambridge, MA: MIT Press)
[22] Falcke M, Huerta R, Rabinovich M I, Abarbanel H D I, Elson R C and Selverston A I 2000 *Biol. Cybern.* **82** 517–27
[23] Destexhe A, Mainen Z F and Sejnowski T J 1994 *Neural Comput.* **6** 14–18
[24] Sharp A A, Skinner F K and Marder E 1996 *J. Neurophysiol.* **76** 867–83
[25] Abarbanel H D I 1996 *Analysis of Observed Chaotic Data* (New York: Springer)
[26] Deco G and Schurmann B 1997 *Phys. Rev. Lett.* **79** 4697–700
[27] Strong S P, Koberle R, de Ruyter van Steveninck R R and Bialek W 1998 *Phys. Rev. Lett.* **80** 197–200
[28] Roulston M S 1999 *Physica* D **125** 285–94
[29] Panzeri S and Treves A 1996 *Network: Comput. Neural Syst.* **7** 87–107
[30] Rieke F, Warland D, de Ruyter van Steveninck R R and Bialek W 1997 *Spikes: Exploring the Neural Code* (Cambridge, MA: MIT Press) section 2.2
[31] Sushchik M, Rulkov N F, Larson L, Tsimring L Sh, Abarbanel H D I, Yao K and Volkovskii A R 2000 *IEEE Commun. Lett.* **4** 128–30